

Application of Vulnerability Determination for Foundation Parameters: A Case Study of Issele- Mkpitime Area of Delta State, Nigeria



Bawallah Musa Adesola^a, Ilugbo Stephen Olubusola^{b*}, Adebayo Babatunde A.^b, Adedapo Johnson Olumide^c, Ofomola Merrious Oviri^d, Oladeji Johnson Femi^e, Raji Idowu^f, Chinyem Felix Iwebunor^d, Hadiza Mali Bukar^g, Bello Kingdom^h, Imolore Mark Ohis^e

^a Department of Applied Geophysics, Federal University of Technology Akure

^b Department of Physics, Lead City University Ibadan

^c Department of Minerals and Petroleum Engineering Technology, Federal Polytechnic, Ado Ekiti

^d Department of Applied Geophysics, Delta State University, Abrakah Nigeria

^e Department of Applied Geology, Federal University of Technology Akure

^f Department of Statistics, Federal University of Technology Akure

^g Department of Political Science and Admin, Yobe State University, Damaturu

^h School of Logistics and Innovation Technology

*Corresponding Author Email: bussytex4peace44@gmail.com, ilugbo.stephen@lcu.edu.ng

DOI: 10.2478/pjg-2021-0009

Abstract:

An integrated geophysical study has been carried out for the evaluation of geological factors that are responsible for foundation stability and vulnerability to failure in a typical sedimentary environment. This is a direct consequence of structural failure that was becoming a matter of almost daily occurrence, especially during the rainy season. In carrying out this study, seven electromagnetic profiles, magnetic as well as Lateral Horizontal Profiling (LRP) were carried out and complimented with Vertical Electrical Sounding (VES). The profiling allowed for the structural delineation of the areas into weak, fairly weak, fairly competent, competent, and very competent zones, while the Vertical Electrical Sounding (VES) delineated the subsurface layer parameters into topsoil, clay horizon, sand, and resistive sand. The vulnerability factors obtained from the statistical analysis were used to determine the stability and generate standardize threshold values. Therefore, since the load-bearing capacity of the foundation of this area is largely dependent on the second layer which is highly incompetent from this study, it then becomes imperative that the ingenuity of the construction/civil engineer must be brought into bearing for the sustainability and stability of any structure in this study area. All the methods engaged in this study exhibits an effective correlation and the area could be inferred/observed to be highly vulnerable to failure as a result of the inherent weak nature of the study location.

Keywords: VLF-EM, Magnetic, VES, Vulnerability, Integrity

1.0. Introduction:

A considerable number of researchers have worked on foundation vulnerability, integrity, soil strength, structural stability, and fundamental issues with regards to functional parameters of foundation soil properties that are majorly responsible for most foundation failures [1-6]. This has become necessary, because engineering structures, i.e. foundation materials are designed and constructed in such a way to allow for long life expectancy. This is not only for the huge financial investment that is involved but for the many consequences that are associated with failures of any dimension including loss of life [7-12]. Therefore, all engineering structures, irrespective of the material that is used for construction must rest upon a competent layer. This foundation is usually underlain or supported by soils and rocks. Hence, the design of the integrity of the foundation and the durability of the structures is extremely dependent on the competency of the soil and rock materials that are situated at where it is being founded [13-19]. It is very worrisome that in recent times, the rate of failure of structures such as roads, dams, buildings, and bridge dimensions in this part of the world especially in Nigeria in recent years. This has made the continuous research about foundation studies and all the dynamics therein an inevitable option in Africa, in an attempt to save more lives and ensure the safety of properties, as well as secure our environment [20-22]. In this present study, the geophysical approach has been adopted. This is because the use of geophysical studies over the year in foundation studies are cheap, fast, and very effective means of delineating and evaluating the subsurface geological structures, their physical parameter, geological settings/layer stratifications, as well as structural trends all of which are factors that are directly responsible for foundation integrity or otherwise [23-24]. Therefore, geophysical methods such as magnetic, Very Low Frequency Electromagnetic (EM), and Electrical Resistivity methods have been deployed in carrying out the evaluation of geological factors that are responsible for foundation stability and vulnerability to failure in a typical sedimentary environment.

2.0. Site Description and Geology of the Study Area

The Issele- Mkpitime area covers a large expanse of land near the Igbodo border (Figure 1). The Issele-Mkpitime is surrounded by water during the rainy season and lies within the northern flank of the Niger Delta basin and it falls within the localities where the lithofacies of the Anambra basin extends and Ogwashi-Asaba Formation which is the lateral equivalent of the Upper Agbada Formation of the Niger Delta. The geology of the Niger Delta has been extensively investigated and recorded by various researchers including [25-28]. The Niger Delta Basin consists of three diachronous siliciclastic or lithostratigraphic units: the deep marine pro-delta Akata Formation, the shallow-marine delta-front Agbada Formation, and the continental delta-top Benin Formation. The study location falls within the Bendel Ameki Formation (Figure 2).

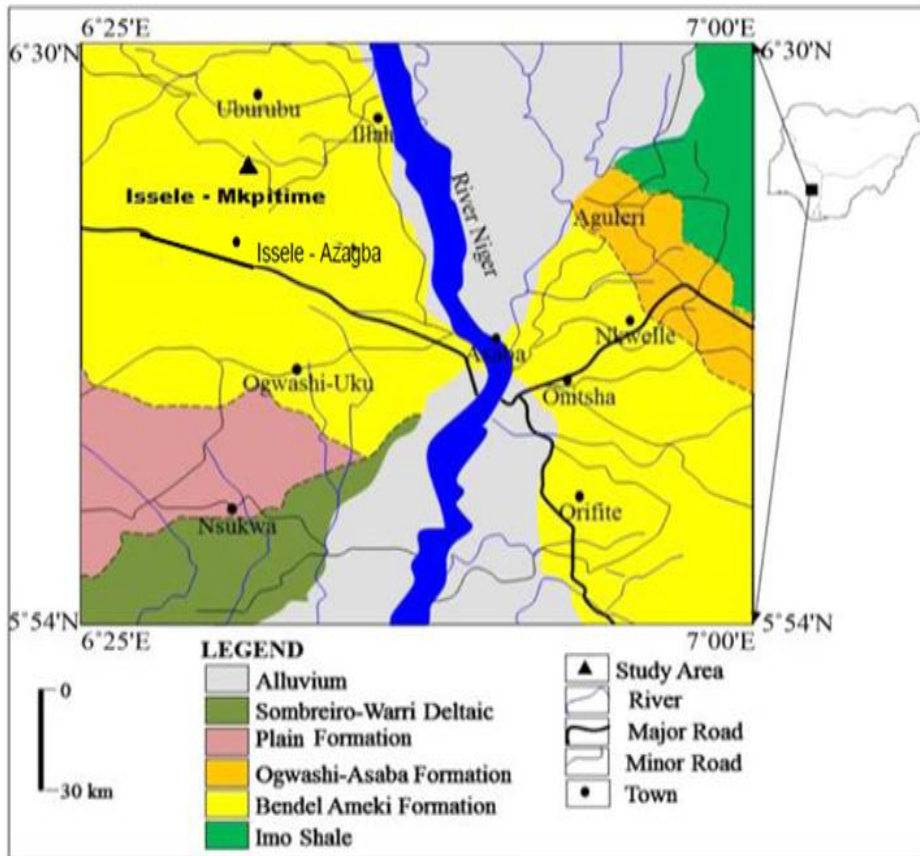


Figure 2. Geological Map of Niger Delta Showing the Study Area

3.0. Research Methodology

Integrated geophysical methods involving the magnetic, Electrical Resistivity, and Very low Frequency Electromagnetic methods were adopted in this research. Seven traverses were established in the West-East direction shown on the base map (Figure 3). The Proton Precision Magnetometer was used for measuring the total field magnetic intensity in nT (nanoTesla). Two Electrical Resistivity techniques were used, the Lateral Horizontal Profiling (LHP) technique and the Vertical Electrical Sounding (VES), for the LHP, the Wenner electrode configuration of station separations and electrode spacing of 20 m. A total of nine (9) VES was carried out in the study area, with the maximum AB/2 being 100 m and minimum of 65m. The Very Low Frequency electromagnetic data was acquired using ABEM WADI VLF equipment with a 20 m station interval on each traverse of varying length. The frequency of operation was 18.0 kHz for the traverses. The parameters measured are raw real, filtered real, raw imaginary, and filtered imaginary components of the electromagnetic field. The following filter operator was used to compute Fraser Filter (Q) to increase the signal to noise ratio of the data set and enhance the anomaly signature, the measured VLF data was subjected to filtering [29].

$$Q = (Q_4 + Q_3) - (Q_2 + Q_1) \tag{1}$$

Where Q is EM data and the subscript are station positions. Karous and Hjelt, 1983, was used to transform the data set to the filtered real VLF data from the application of equation (1) on real component VLF, then plotted using excel word spread sheet. The apparent resistivity is plotted versus AB/2 in meters on bilogarithmic paper resulting in a VES curve. The VES curve showed the change of resistivity with a depth, since the effective penetration increases with increasing electrode spacing. The interpretation of the VES curve is both qualitative and quantitative that is based upon an algorithm of [30-35]. The quantitatively interpreted sounding curves gave interpreted results as geoelectric parameters (that is, layer resistivity and layer thickness). All the three methods were determined statistically and integrated to evaluate geological factors that are majorly responsible for foundation vulnerability and stability. Also, to determine the standard threshold values for site construction purposes

The Below equation was generated to determine threshold values:

$$\text{Vulnerability index} = A \tag{2}$$

Where A = addition of all the weak zones divided by the total distance multiply by 100

$$\text{Stability Index} = B \tag{3}$$

where B = subtraction of vulnerability index value from 100%

$$\text{Threshold Values} = B/A \tag{4}$$

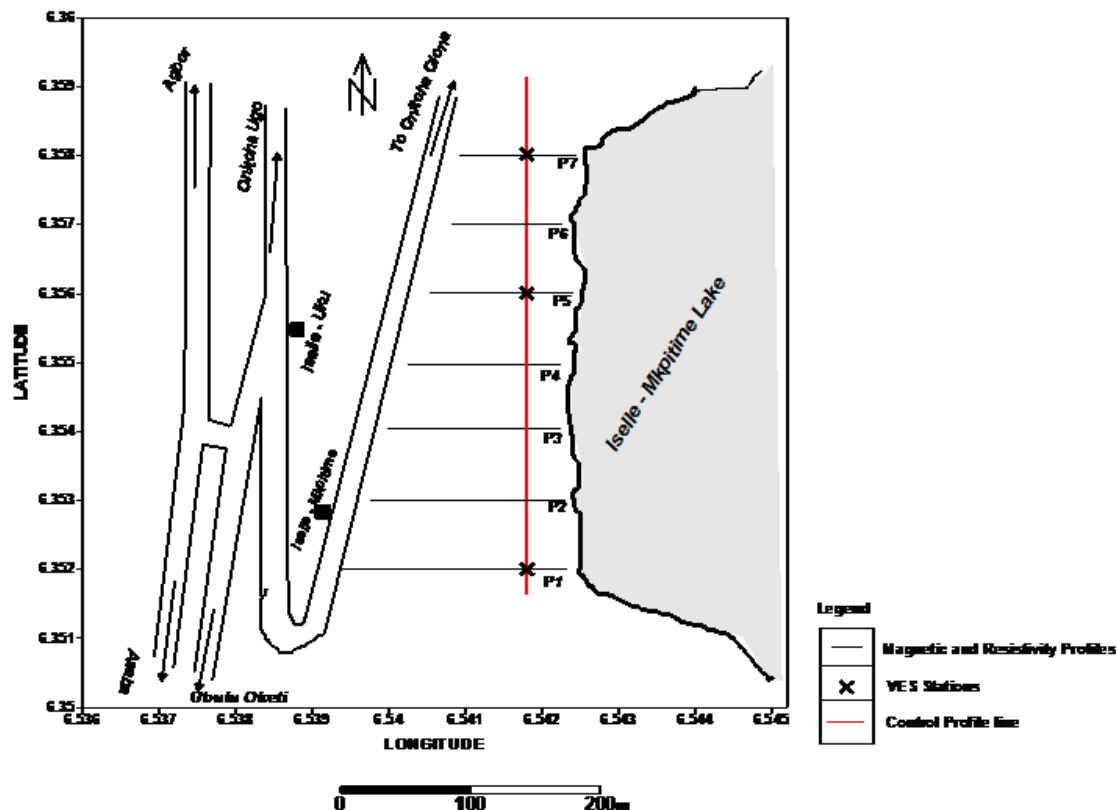


Figure 3. Acquisition Map of the Study area

4.0. Results and Discussion

4.1. VLF-EM

4.1.1. Profile one

Figure 4 shows the VLF-EM profile along traverse one in E-W direction covering a distance of 500 m. The major anomalous zone (weak region) of interest were observed at a distance between zero to 120 m, 240 to 260 m, and 360 to 480 m; cover at a total distance of about (120 m + 20 m + 120 m) i.e. 260 m when compared statistically with the total length of the traverse, the percentage vulnerability of the structural parameters to failure is given as $260/500 \times 100 = 52\%$

Since the vulnerability is 52%, then stability along the profile was;

$$\text{Stability} = 100 - 52\% = 48\%$$

$$\text{The threshold} = \text{Stability}/\text{Vulnerability} = 48 / 52 = 0.92$$

This implies that the subsurface properties along profile one is highly vulnerable to failure

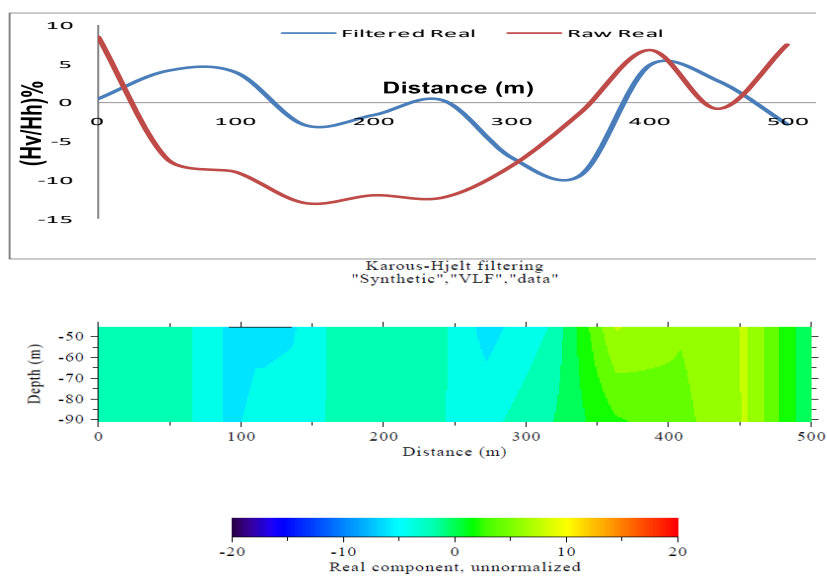


Figure 4. VLF-EM along Profile one

4.1.2. Profile two

The VLF-EM profile along traverse two cover a distance of about 400 m and is taken from the E-W direction (Figure 5). Seven anomalous regions of weak geologic/soil materials, these zones were identified at 30 to 60 m, 80 to 110 m, 180 to 240 m, 260 to about 290 m, from 320 to about 340 m, 360 to 400 m, which were summed up to be 30 + 30 + 60 + 30 + 20 + 40 m = 210 m. when compared with the total distance of about 400 m.

Statistically; $210/400 \times 100 = 52.5\%$

Therefore, the EM vulnerability factor of the soil vulnerability to failure along profile two is 52.5%

Since the vulnerability is 52.5 %, then stability along the profile was;

Stability = $100 - 52.5 \% = 47.5 \%$

The threshold = $\text{Stability}/\text{Vulnerability} = 47.5 / 52.5 = 0.91$

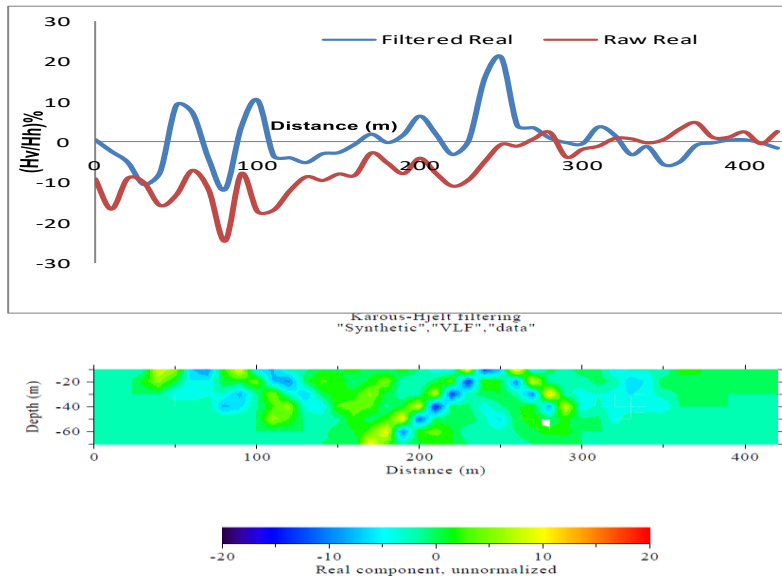


Figure 5. VLF-EM along Profile Two

4.1.3. Profile three

The VLF-EM along profile three covers a distance of 600 m, taken across E-W direction (Figure 6), the EM response from the study area ranged between 32% and -22%; reflecting the nature of the positive and negative anomaly i.e. the conductive (weak) zones and the non-conductive (competent/resistive materials). Seven regions/zones of a positive anomaly of interest depicting regions/zones of weak geologic materials were identified. These were located at 50 to 60 m, 100 to 150 m, 180 to 400 m, 440 to 550 m, and 570 to 590 m, representing intervals of 10 + 50 + 220 + 110 + 20 m when compared with the total profile distance and the percentage vulnerability of the subsurface soil materials is given as $410/600 \times 100 = 67.3\%$.

Since the vulnerability is 67.3 %, then stability along the profile was;

Stability = $100 - 67.3 \% = 32.7 \%$

The threshold = $\text{Stability}/\text{Vulnerability} = 32.7 / 67.3 = 0.49$

The implication of this is such that the subsurface soil stability of this profile located within the study area is very low, implying a high vulnerability to failure.

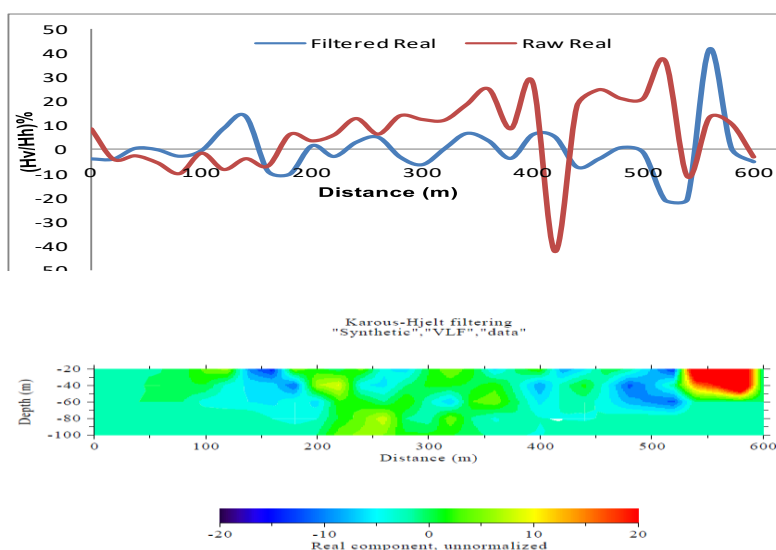


Figure 6. VLF-EM along Profile Three

4.1.4. Profile four

VLF-EM profile four, the EM measurement of profile four cover a distance of about 600 m and is taken from the E-W direction (Figure 7). The variation in EM readings varies between 33% to -38% indicative of both positive and negative anomalous zones, depicting the presence of both weak and competent geologic materials [36-41]. The regions characterized by positive anomaly areas are indicative of weak geologic materials while areas with negative anomaly depict a region of resistive geologic materials/competent zones. These zones of positive anomalies of interest were identified from this profile. These were between zero to about 150 m, 320 to 450 m, and 540 to 600 m, representing intervals of 150 + 130 + 60 m = 440 m, when compared with the total distance of 600 m. the vulnerability factor in term of percentage is; $440/600 \times 100 = 73.2\%$

Since the vulnerability is 73.2 %, then stability along the profile was;

$$\text{Stability} = 100 - 73.2 \% = 26.8 \%$$

$$\text{The threshold} = \text{Stability}/\text{Vulnerability} = 26.8 / 73.2 = 0.37$$

This implies that the profile depicts a region of high vulnerability in terms of the geologic materials making up the subsurface materials along with this profile and this implies geologic materials of very low subsurface stability.

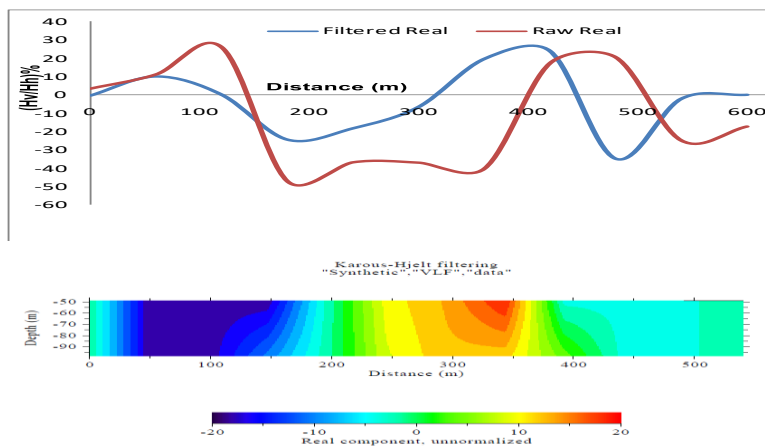


Figure 7. VLF-EM along Profile Four

4.1.5. Profile five

VLF-EM along profile five covers a distance of about 260 m (Figure 8). The zones of positive anomalies of interest were identified from the profile. These occurred at between 10 to 70 m, 80 to 100 m, and 170 to 260 m. this reflects an interval of 60 + 20 + 90 m = 170 m, when compared with the total distance covered, the percentage vulnerability factor is considered to be $170/260 \times 100 = 65.7\%$

Since the vulnerability is 65.7 %, then stability along the profile was;

$$\text{Stability} = 100 - 65.7 \% = 34.3 \%$$

$$\text{The threshold} = \text{Stability}/\text{Vulnerability} = 34.3 / 65.7 = 0.52$$

This reflects a high degree of subsurface vulnerability to failure and hence subsurface soil materials of very low subsurface stability.

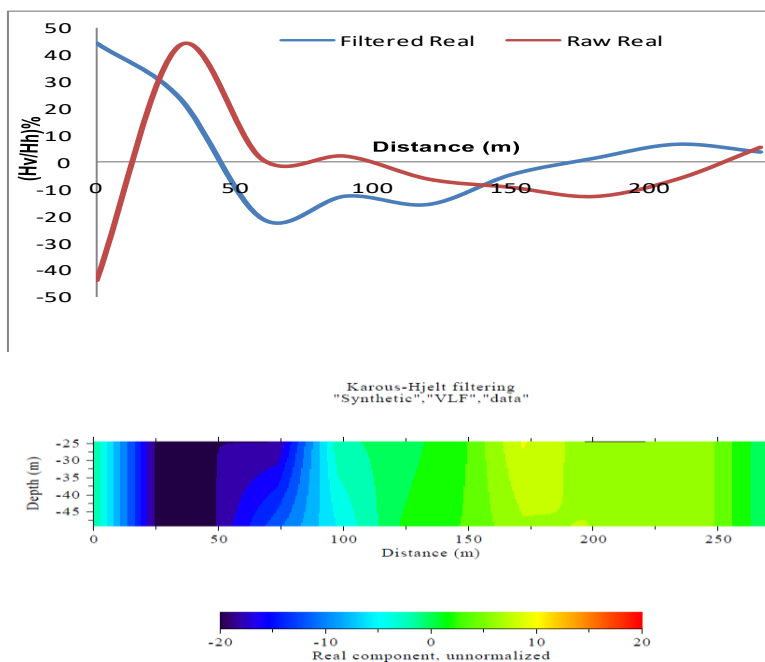


Figure 8. VLF-EM along Profile Five

4.1.6. Profile Six

VLF-EM profile six was taken along the E-W direction (Figure 9). It covers a distance of about 400 m, with variation in EM measurement ranging between 14.2 % and -18.6% reflecting the changes in lithology, soil integrity vulnerability indicative of the existence of both weak and competent zones. However, the major points of interest to this study area region of positive and negative anomaly, most especially regions of positive anomaly which are directly related to weak zones or regions associated with vulnerability. Subsequently, six anomalous zones of interest were identified along this profile. These were obtained between zero to about 20 m with values ranging between 0.2 and less than 1%. The second point of positive anomaly (weak) zone was found between 60 to 70 m, covering a lateral extent of about 10 m, while another zone was obtained between 90 to 130 m with reading ranging between 0.1% to about 14.4%, covering a lateral extent of about 40 m. Furthermore, another anomalous zone of interest was observed between 260 to 350 m with EM reading ranging between 0.1% to 9.6% and covering a distance of about 90 m in extent.

The total distance (lateral extent) of the anomalous zone was compared with the total distance of the entire profile which can be considered as $160/400 \times 100 = 40\%$.

Since the vulnerability is 40 %, then stability along the profile was;

$$\text{Stability} = 100 - 40 \% = 60 \%$$

$$\text{The threshold} = \text{Stability}/\text{Vulnerability} = 60 / 40 = 1.5$$

Therefore, it can be inferred that 40% of the entire profile six is faced with the challenges associated with weak zone i.e. vulnerability to failure, implying subsurface material of low integrity, while 60% of the entire profile was stable in terms of subsurface soil integrity and hence, low vulnerability.

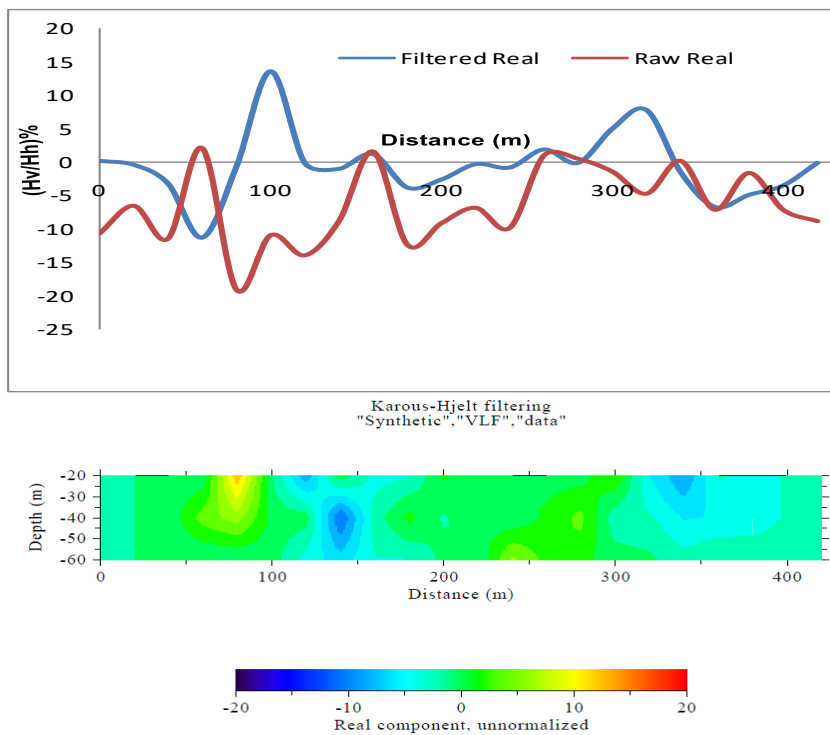


Figure 9. VLF-EM along Profile Six

4.1.7. Profile seven

VLF-EM profile along traverse seven covers a distance of 250 m (Figure 10), EM measurement was carried out along E-W orientation. The EM measurement varied between 6.85 to 17.6% and the entire profile was characterized by positive anomaly, which implies a percentage of 100% indicative of subsurface geologic materials along the entire profile seven to be very low integrity as well as high vulnerability to failure

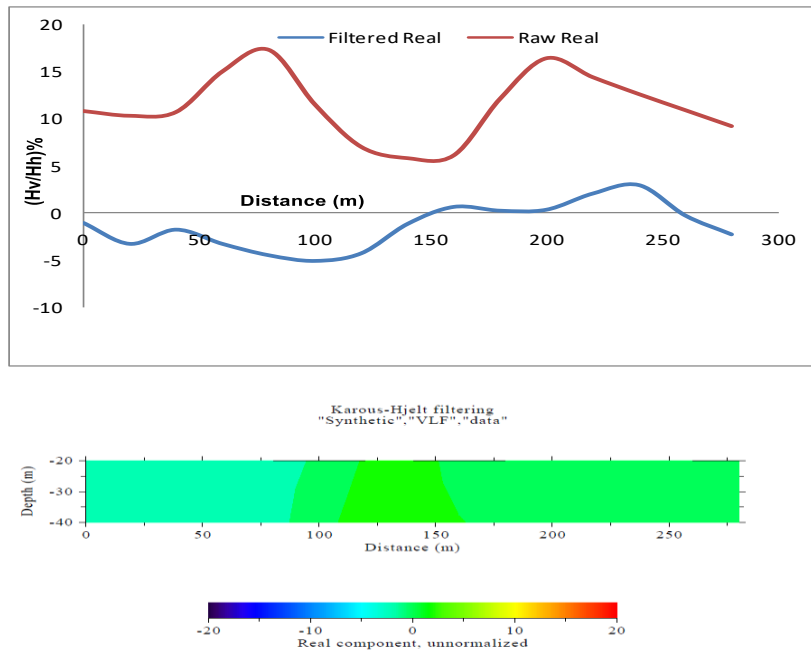


Figure 10. VLF-EM along Profile Seven

4.2. Magnetic Method

4.2.1. Profile one

The magnetic profile along traverse one covers a total distance of 500 m which was taken concurrently along with EM profiles (Figure 11). Five major anomalous zones of interest which represent regions of low magnetic susceptibility indicative of the region of weak geologic materials were identified, between zero origin to 30 m, 60 to 110 m, 180 to 280 m, 350 to 430 m, and 450 to 500 m. representing 30 m, 50 m, 100 m, 80 m, and 50 m, making a total lateral extent of 310 m, when compared with the total traverse distance of 500 m. it can be determined nor inferred that the vulnerability in terms of percentage

$$= 310/500 \times 100 = 62\%$$

Since the vulnerability is 62 %, then stability along the profile was;

$$\text{Stability} = 100 - 62 \% = 38 \%$$

$$\text{The threshold} = \text{Stability}/\text{Vulnerability} = 38 / 62 = 0.61$$

This implies that this profile is characterized by materials of low stability and high vulnerability.

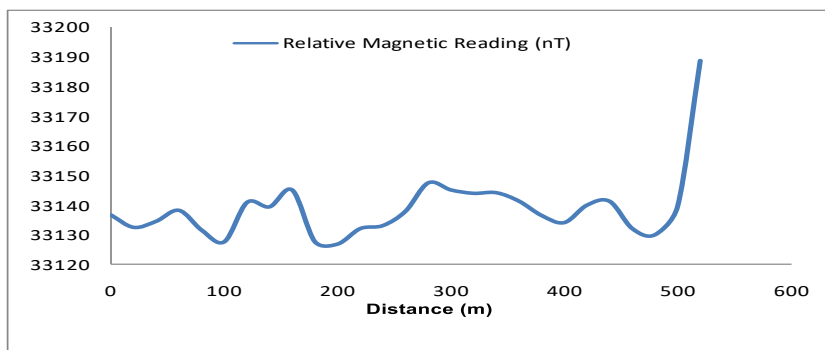


Figure 11. Magnetic Profile along Profile One

4.2.2. Profile two

The relative magnetic reading along traverse two was taken across the E-W direction concurrently along the EM profile (Figure 12). It covers a distance of about 500 m. the reading obtained varied between 33120 to 33150 nT, reflecting the magnetic susceptibility of the subsurface geologic materials which was characterized by moderately low magnetic susceptibility with variations in the trend of the anomaly that obtained along the profile of study. Six anomalous zones were observed along the profile with varying lateral extent between 20 to 50 m, 80 to 100 m, 110 to 200 m, 220 to 240 m, 250 to 330 m, 350 to 400 m, and 410 to 500 m representing the lateral extent of 30 + 20 + 90 + 20 + 80 + 50 + 90 respectively, making a cumulative distance of 380 m. therefore, when compared as a percentage against the total distance of 500 m, the vulnerability factor in terms of the subsurface soil integrity is equal $380/500 \times 100 = 76\%$

Since the vulnerability is 76 %, then stability along the profile was;

$$\text{Stability} = 100 - 76 \% = 24 \%$$

$$\text{The threshold} = \text{Stability}/\text{Vulnerability} = 24/76 = 0.32$$

This is indicative of a high degree of vulnerability to failure as well as reflecting subsurface geologic materials of very low stability.

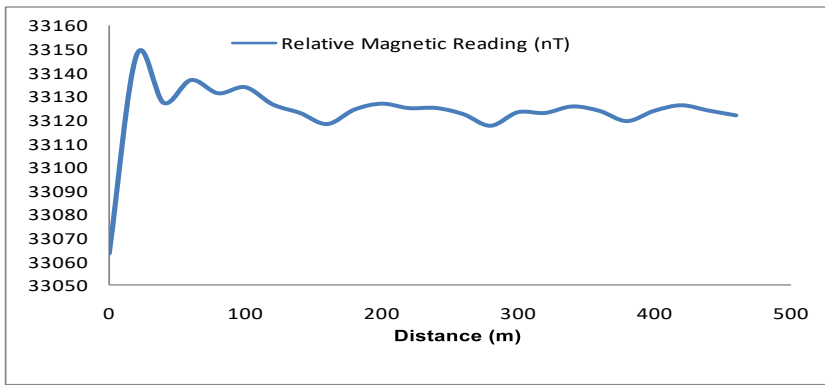


Figure 12. Magnetic Profile along Profile Two

4.2.3. Profile three

Relative magnetic reading along traverse three covers a total distance of 400 m (Figure 13), the traverse was taken E-W direction. The measurement obtained exhibits varied magnetic susceptibility contrasts reflecting variations in subsurface lithology and layer stratification along this profile. The measurement varied between 33045 nT and 33085 nT, with various susceptibility anomalies, with the interest of study here being areas/region associated with low susceptibility contrast, depicting weak zones associated with vulnerability nor regions of low foundation integrity. These were identified in Eight (8) locations i.e. at zero to 20 m, 50 to 70 m, 100 to 120 m, 120 to 220 m, 240 to 250 m, 280 to 340 m, 350 to 380 m and 390 to 400 m representing lateral extent of $20 + 20 + 20 + 100 + 10 + 60 + 30 + 10 = 270$ m.

Therefore, vulnerability factor as a percentage = $270/400 \times 100 = 67.5\%$

Since the vulnerability is 67.5 %, then stability along the profile was;

Stability = $100 - 67.5 \% = 32.5 \%$

The threshold = $Stability/Vulnerability = 32.5 / 67.5 = 0.48$

This exhibits that subsurface geologic material has low stability and high vulnerability typically of clay or shale top horizon sedimentary environment

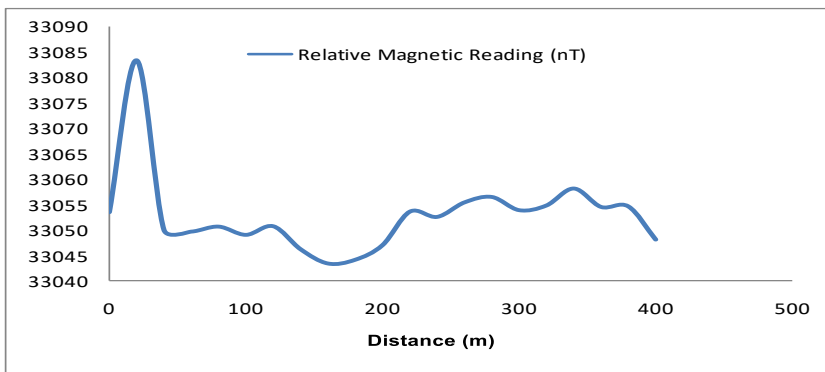


Figure 13. Magnetic Profile along Profile Three

4.2.4. Profile four

Magnetic reading along profile four covers a distance of 350 m and measurement was conducted along E-W direction (Figure 14). The measurement was characterized by varying magnetic susceptibility which varies between 33110 to 33125 nT reflecting the variations in subsurface geologic materials within the study area. six anomalous zones of interest were identified along the profile, which ranges from zero to 40 m, 70 to 90 m, 100 to 200 m, 230 to 300 m and 330 to 350 m; reflecting lateral extent of $40 + 20 + 100 + 70 + 20 = 250$ m and vulnerability factor of $250/350 \times 100 = 71.6\%$,

Since the vulnerability is 71.6 %, then stability along the profile was;

Stability = $100 - 71.6 \% = 28.4 \%$

The threshold = $Stability/Vulnerability = 28.4 / 71.6 = 0.40$

This indicates that the subsurface soil materials display low foundation stability and high vulnerability.

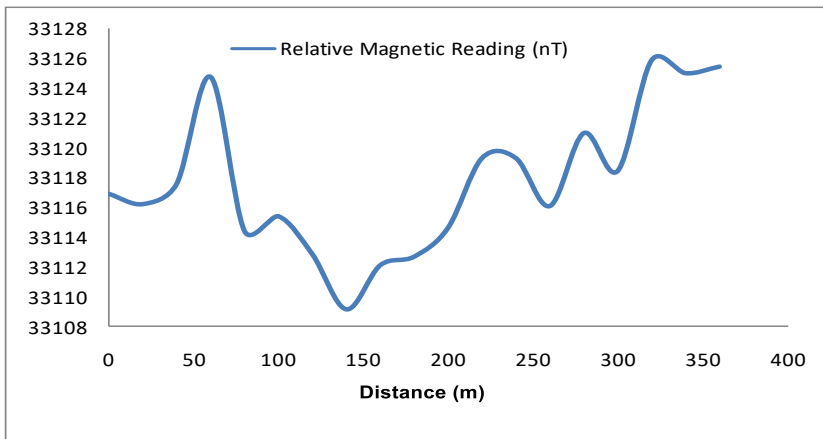


Figure 14. Magnetic Profile along Profile Four

4.2.5. Profile five

The relative magnetic reading of profile five covers a distance of 350 m. the measurement along with others was carried out concurrently along with the EM profile (Figure 15). The magnetic readings varied between 33102 nT and 33118 nT, with about eight regions of anomalous interest which reflects the variation in subsurface geology of the study area. These anomalous zones was obtained between zero to 20 m, 40 to 70 m, 90 to 120 m, 140 to 160 m, 180 to 200 m, 210 to 240 m, 270 to 300 m, and 320 to 350 m. reflecting $20 + 30 + 30 + 20 + 20 + 30 + 30 + 30 = 210$ m, which indicate of subsurface geologic material of low foundation integrity and high vulnerability to failure.

The vulnerability factor = $210/350 \times 100 = 60\%$

Since the vulnerability is 60 %, then stability along the profile was;

Stability = $100 - 60\% = 40\%$

The threshold = $Stability/Vulnerability = 40 / 60 = 0.67$

This indicates that the subsurface soil materials display low foundation stability and high vulnerability.

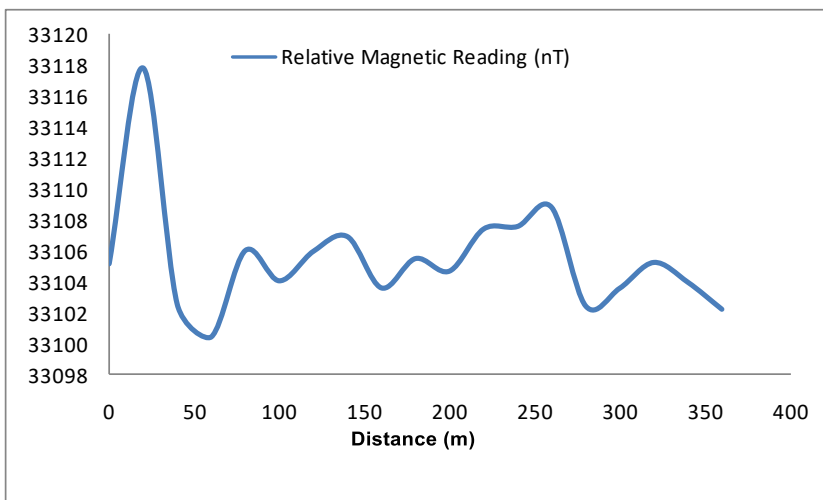


Figure 15. Magnetic Profile along Profile Five

4.2.6. Profile six

The measurement along profile six covers a distance of 250 m (Figure 16), it was taken along the E-W direction with the reading obtained ranging between 33080 nT and 33130 nT. Six anomalous zones of interest were observed along this profile. These were identified between 10 to 30 m, 50 to 70 m, 80 to 100 m, 120 to 170 m, 190 to 230 m and 240 to 250 m; reflecting $20 + 20 + 20 + 30 + 40 + 10 = 140$ m. the total anomalous extent was compared with the total profile distance of 250 m. the vulnerability factor becomes; $140/250 \times 100 = 56\%$, which implies moderately foundation vulnerability factor which reflects subsurface material of moderate foundation integrity.

Since the vulnerability is 56 %, then stability along the profile was;

Stability = $100 - 56\% = 44\%$

The threshold = $Stability/Vulnerability = 44 / 56 = 0.79$

This indicates that the subsurface soil materials display low foundation stability and high vulnerability.

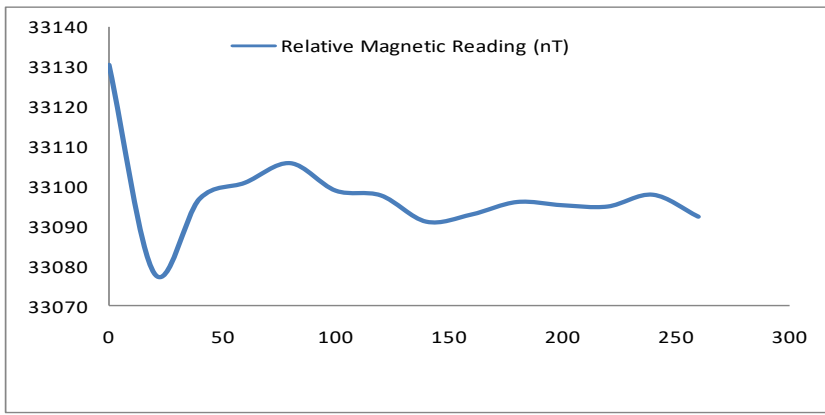


Figure 16. Magnetic Profile along Profile Six

4.2.7. Profile seven

The magnetic measurement along profile seven covers a distance of 300 m (Figure 17), which was taken across the E-W direction with magnetic reading varying between 33080 nT and 33090 nT; reflecting the varying lithology and subsurface layer stratification within the study area. five anomalous zones of interest were identified along this profile, these obtained between zero to 30 m, 60 to 90 m, 110 to 130 m, 160 to 210, and 260 to 300 m; reflecting a total lateral extent of $30 + 30 + 20 + 50 + 40 \text{ m} = 170 \text{ m}$ i.e. $170/300 \times 100 = 56.7\%$. This is indicative of subsurface geologic materials characterized by very high foundation vulnerability as well as foundation materials with very low/extremely poor integrity.

Since the vulnerability is 56.7 %, then stability along the profile was;

$$\text{Stability} = 100 - 56.7 \% = 43.3 \%$$

The threshold = $\text{Stability}/\text{Vulnerability} = 43.3/56.7 = 0.76$. This indicates that the subsurface soil materials display low foundation stability and high vulnerability.

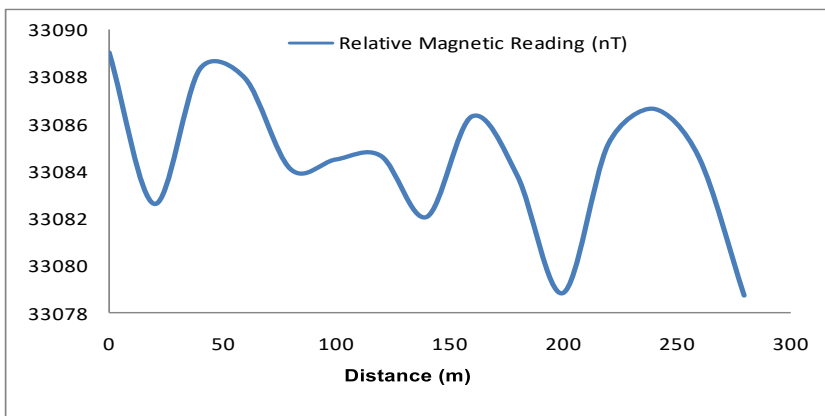


Figure 17. Magnetic Profile along Profile Seven

4.3. Lateral Horizontal Profiling

4.3.1. Profile one

The lateral horizontal profiling (LRP) along traverse one covers a distance of about 400 m in the E-W direction (Figure 18), with resistivity variation ranging between 100 to 1400 Ωm . The measurement obtained reflects variation in lithological comprises of the subsurface geologic material which reduces with distance along this profile. The principle here is such that the lower the resistivity, the higher is the vulnerability factor for failure and the lower the subsurface integrity. Therefore, the midpoint between the highest and lowest resistivity values was adopted as a controlling factor in the determination of the vulnerability factor along the resistivity processes. Subsequently, this point was projected and obtained to fall within and at about 150 m on the horizontal distance. The total distance gives the vulnerability factor of the profile to be; $250/400 \times 100 = 62.5\%$, depicting a high vulnerability factor as well as subsurface materials of low integrity.

Since the vulnerability is 62.5 %, then stability along the profile was;

$$\text{Stability} = 100 - 62.5 \% = 37.5 \%$$

The threshold = $\text{Stability}/\text{Vulnerability} = 37.5/62.5 = 0.6$. This indicates that the subsurface soil materials display low foundation stability and high vulnerability.

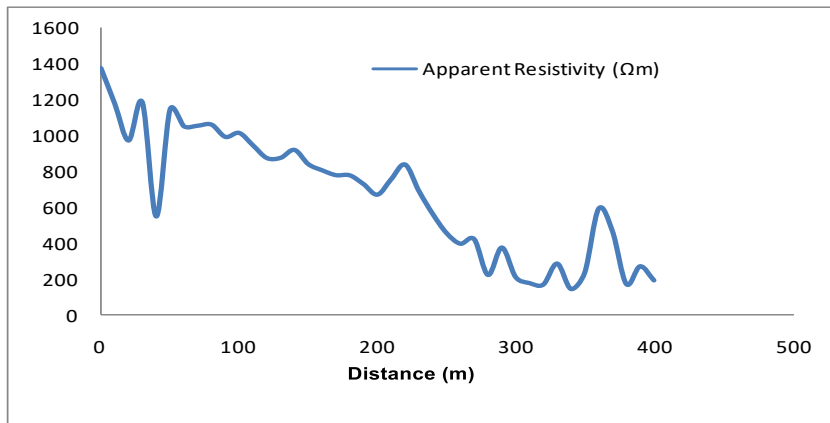


Figure 18. Wenner Horizontal Profiling along Profile One

4.3.2. Profile two

The apparent resistivity measurement of profile two covers a distance of 400 m (Figure 19) with the resistivity values ranging from less than 100 Ωm to a maximum of 1300 Ωm. The midpoint is projected to be at 650 Ωm which was found to be at a distance of about 140 m beyond which the apparent resistivity reduces with depth, while the vulnerability factors are calculated to be; $260/400 \times 100 = 60.5\%$. These are characteristics of the subsurface geologic environment with high vulnerability factor and low integrity.

Since the vulnerability is 60.5 %, then stability along the profile was;

$$\text{Stability} = 100 - 60.5 \% = 39.5 \%$$

The threshold = $\text{Stability}/\text{Vulnerability} = 39.5/60.5 = 0.65$. This indicates that the subsurface soil materials display low foundation stability and high vulnerability.

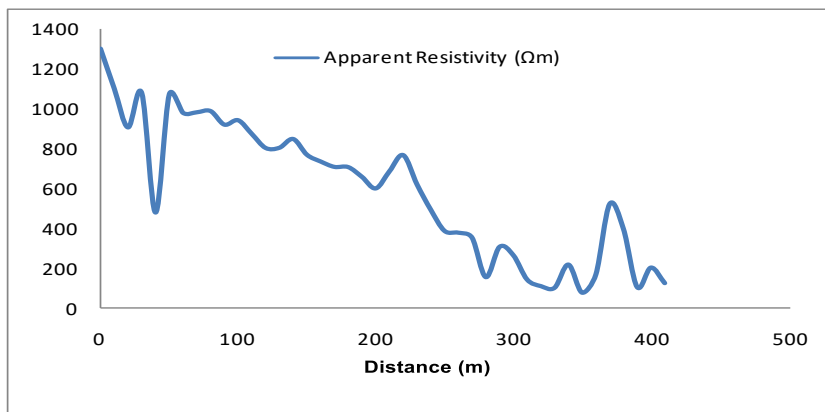


Figure 19. Wenner Horizontal Profiling along Profile Two

4.3.3. Profile three

The lateral resistivity profile of traverse three covers a distance of about 400 m (Figure 20), the measurement was carried out in E-W direction in line with other traverses. The apparent resistivity ranged between less than 200 Ωm to a maximum of 1400 Ωm, reflecting the changes in the subsurface geologic compositions. The profile plot obtained indicated that apparent resistivity along this profile reduces over distances, while the midpoint between the minimum and maximum resistivity along this profile was projected to be at about 180 m, which gives a vulnerability factors over the distance being considered to be $220/400 \times 100 = 55\%$, which was obtained to be indicative of moderately high vulnerability factors as well as of moderately low integrity characteristics of the fairly stable geologic environment in terms of foundation integrity.

Since the vulnerability is 55 %, then stability along the profile was;

$$\text{Stability} = 100 - 55 \% = 45 \%$$

The threshold = $\text{Stability}/\text{Vulnerability} = 45/55 = 0.82$. This indicates that the subsurface soil materials display low foundation stability and high vulnerability.

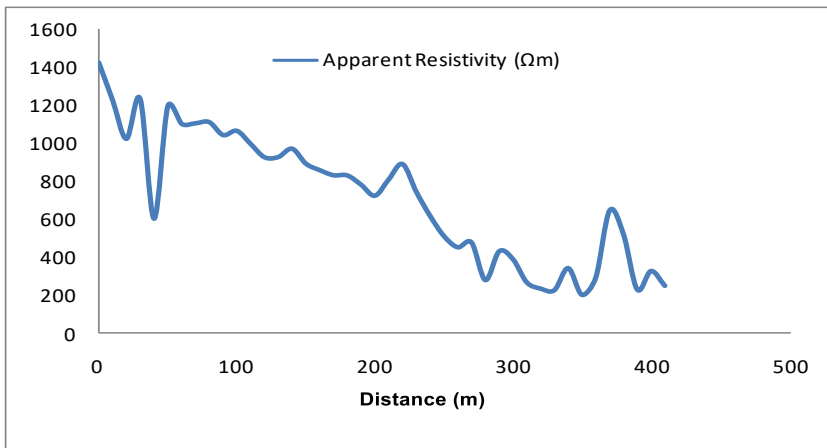


Figure 20. Wenner Horizontal Profiling along Profile Three

4.3.4. Profile four

The apparent resistivity measurement of profile four was carried out along the E-W direction (Figure 21), covering a distance of 400 m. the resistivity response varied between less than 200 Ωm to above 3500 Ωm. The anomalous response obtained from this profile was characterized with very high resistivity from about the origin to a distance of about 50 m, after which a drastic drop with apparent resistivity was observed from about 1000 Ωm; from 3500 Ωm to about 1000 Ωm and continued to drop up to less than 200 Ωm, from a distance of about 250 m to 400 m by extension, the vulnerability factor of this profile was obtained to be $300/400 \times 100 = 70.5\%$ indicative of the existence of geologic material of very low integrity and very high vulnerability to failure i.e. material of high vulnerability factor.

Since the vulnerability is 70.5 %, then stability along the profile was;

$$\text{Stability} = 100 - 70.5 \% = 29.5 \%$$

$$\text{The threshold} = \text{Stability}/\text{Vulnerability} = 29.5/70.5 = 0.42.$$

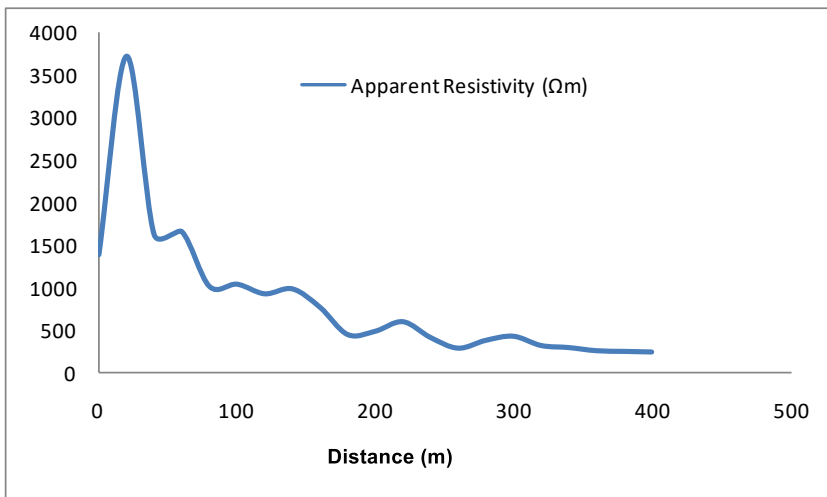


Figure 21. Wenner Horizontal Profiling along Profile Four

4.3.5. Profile five

Similar to the situation obtained in profile four, the apparent resistivity of profile five was characterized majorly by subsurface geologic material of very low integrity and high vulnerability as exhibited by the measurement obtained with resistivity ranging between less than 100 Ωm to as high as 3500 Ωm (Figure 22). The beginning of the profile was characterized by high resistivity of a little above 3500 Ωm which extends up to about 20 m beyond which the resistivity continues to drop. In this profile, the midpoint between the highest and lowest resistivity was obtained to be at 1750 Ωm which projected against the distance. It was found to coincides with about 50 m on the profile when considering the entire profile. The vulnerability factor can then be obtained to be; $350/400 \times 100 = 87.5\%$, this implies that the subsurface geologic material along this profile is of very high vulnerability and hence, very low integrity in terms of soil competence or foundation or founding materials.

Since the vulnerability is 87.5 %, then stability along the profile was;

$$\text{Stability} = 100 - 87.5 \% = 12.5 \%$$

$$\text{The threshold} = \text{Stability}/\text{Vulnerability} = 12.5/87.5 = 0.14.$$

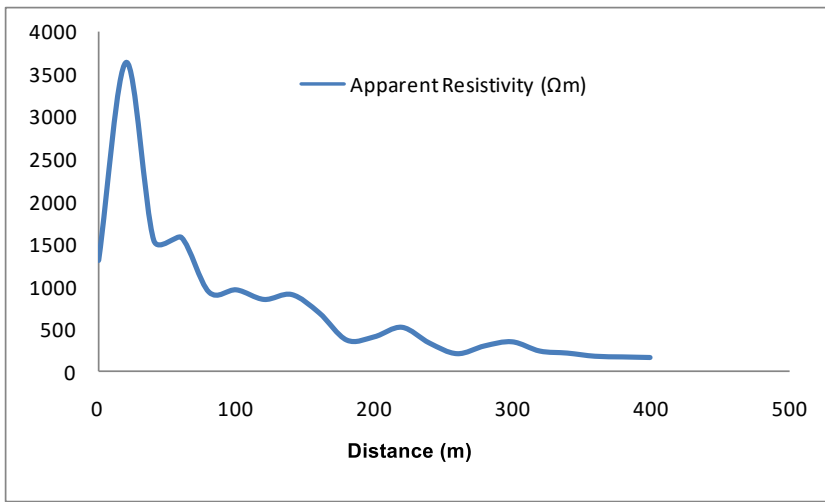


Figure 22. Wenner Horizontal Profiling along Profile Five

4.3.6. Profile six

The apparent resistivity measurement of profile six covers a distance of 400 m and was taken along the E-W direction (Figure 23). The profile was characterized by variation in resistivity which ranges between less than 200 Ωm and 3500 Ωm with the midpoint between the minimum and maximum resistivity being at 1750 Ωm. This translates to about 40 m when projected down along the profile which implies that from zero to about 40 m along the profile was characterized by high resistivity while the rest of the profile exhibits low resistivity from about 40 m to the end of the profile at about 400 m. the estimation of the vulnerability factors can be determined by $360/400 \times 100 = 90\%$, which implies that the profile can be described as highly vulnerable and very low foundation integrity.

Since the vulnerability is 90 %, then stability along the profile was;

$$\text{Stability} = 100 - 90 \% = 10 \%$$

$$\text{The threshold} = \text{Stability}/\text{Vulnerability} = 10/90 = 0.11.$$

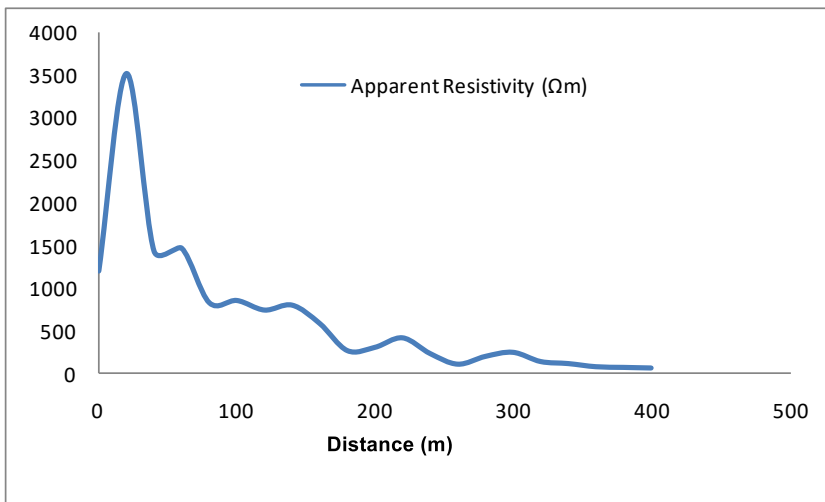


Figure 23. Wenner Horizontal Profiling along Profile Six

4.3.7. Profile seven

The lateral resistivity profile measurement of profile seven was taken along the E-W direction (Figure 24). The profile covers a distance of 300 m with varied apparent resistivity which ranged between less than 200 Ωm to as high as 4500 Ωm. The high resistivity anomalous zone obtained along this profile occurred at a distance of about 40 m and extends up to about 90 m, covering a lateral extent of about 50 m when considered along with the total distance. Therefore, the vulnerability factor can be estimated to be $210/300 \times 100 = 70\%$. Hence, the subsurface geologic material associated with this profile can be said to be of low foundation integrity because of its high integrity.

Since the vulnerability is 70 %, then stability along the profile was;

$$\text{Stability} = 100 - 70 \% = 30 \%$$

$$\text{The threshold} = \text{Stability}/\text{Vulnerability} = 30/70 = 0.43.$$

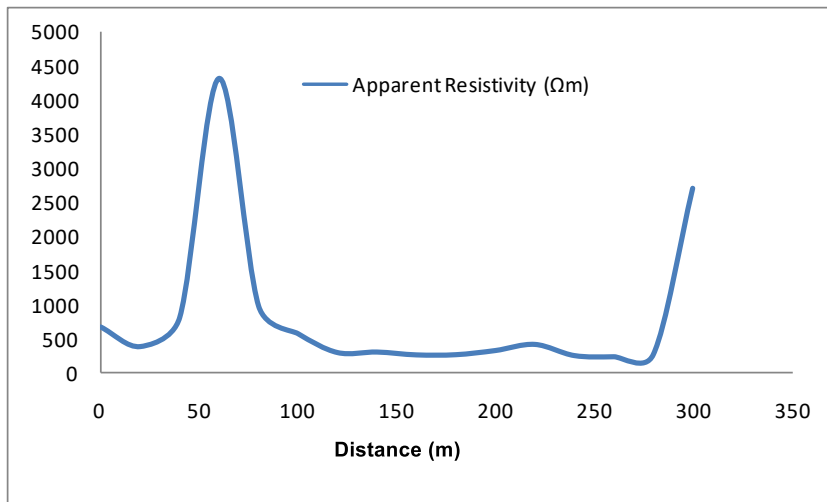


Figure 24. Wenner Horizontal Profiling along Profile Seven

4.4. Comparisons of the Vulnerability Factors for the three Methods

This implies that almost all the entries subsurface geologic environment within the study area is very vulnerable and of very low foundation integrity. Hence, the ingenuity required from constructions and civil engineers to put in place a structure that we overcome the geologic defects that may pose a major threat to structures. Comparing the vulnerability factors resulting from each of the methods that were deployed:

$$EM = 52+52+5+67.3+73.2+65.7+40+100/7 = 64.4\%$$

$$Magnetic = 62+76+67.5+71.6+60+56+90/7 = 67.2\%$$

$$LHP = 60+60.5+55+70.5+87.5+90+70/7 = 70.5\%$$

Therefore, the vulnerability factors derive from the three approaches that were deployed were of the order of 64.4%, 67.2%, and 70.2% respectively, which implies that the study area is highly vulnerable to fail.

A standard threshold value was determined for future researchers on foundation construction in terms of geophysical investigation (Table 1). These threshold values must be complemented with engineering geotechnical investigation to ascertain a standardized measure for construction purposes.

Table 1. Threshold Values Classification for Site Construction Purposes

Threshold Values	Classification	Stability (%)	Vulnerability (%)
< 1	Extremely Low	Stability is less than 50%	Vulnerability is more than 50%
1 - 3	Low	Stability is less than 70%	Vulnerability is more than 30%
4 - 9	Moderate	Stability is less than 90%	Vulnerability is more than 10%
>10	High	Stability greater than 90%	Vulnerability is less than 10%

4.5. Vertical Electrical Sounding

The vertical electrical sounding was carried out within the study area, further assisting in the understanding the subsurface configuration, lithological variations as well as the geoelectric sequence of the entire study area for a better assessment of the subsurface geology. To be able to achieve this; nine (9) VES were carried out in order of three VES in each profile 1, 5, and 7 respectively, upon which the geoelectric section across each of these profiles was generated.

4.5.1. Characteristic of the VES Curves

Curves types identified range from H and KH varying between three to four geoelectric layers. The H curve type predominates. Typical curve types in the area are as shown below (Figure 25).

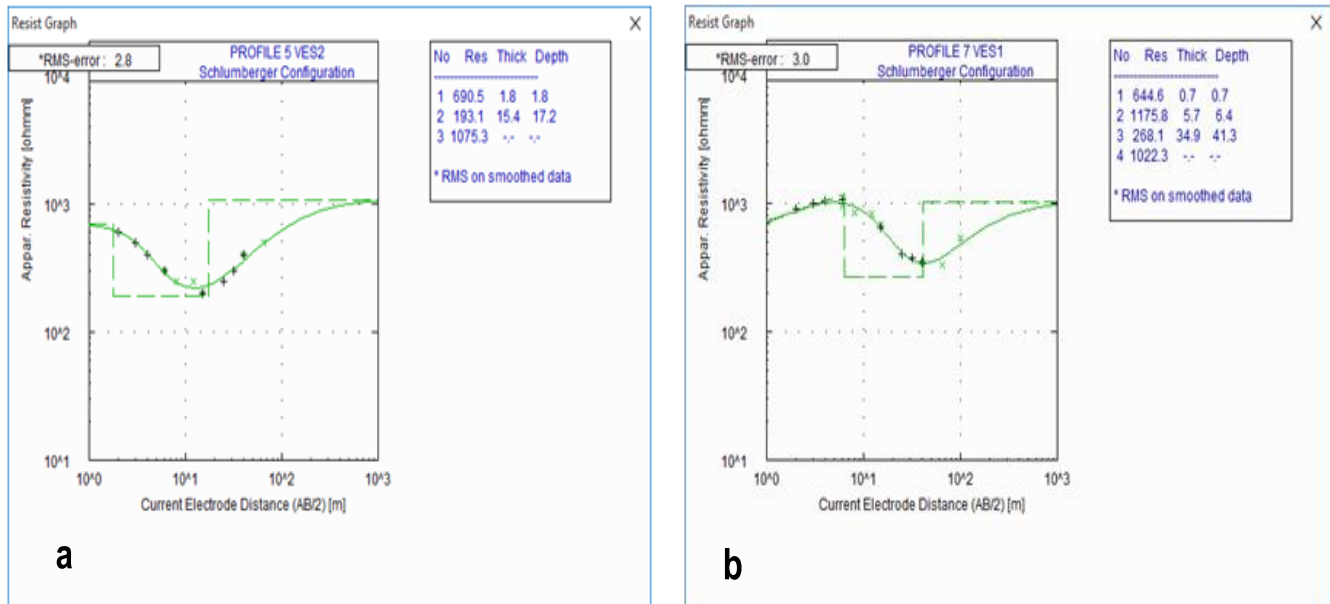


Figure 25. Typical Curve Types (a) H (b) KH

4.5.2. Geoelectric Section

4.5.2.1. Geoelectric Section along Profile One

Three distinctive geoelectric sequences were observed along with this profile (Figure 26). These comprise of the topsoil with layer resistivity ranging from 794 to 1157 Ω m and layer thickness varies from zero to about 2.0 m. the second layer which is considered here as the major layer of interest is characterized by layer resistivity ranging from 96 to 144 Ω m which is characterized of the weak zone, made up of predominantly highly vulnerable shale or clay geologic materials which effectively confirms the effectiveness of the earlier three methods engaged in the studies of the nature. The layer thickness of this formation ranged between 2.0 to about 16 m, while the third layer delineated is characterized by layer resistivity and thickness ranging from 281 to 353 Ω m and 10 m and above, which is characterized by moderate/partly resistive sand formation.

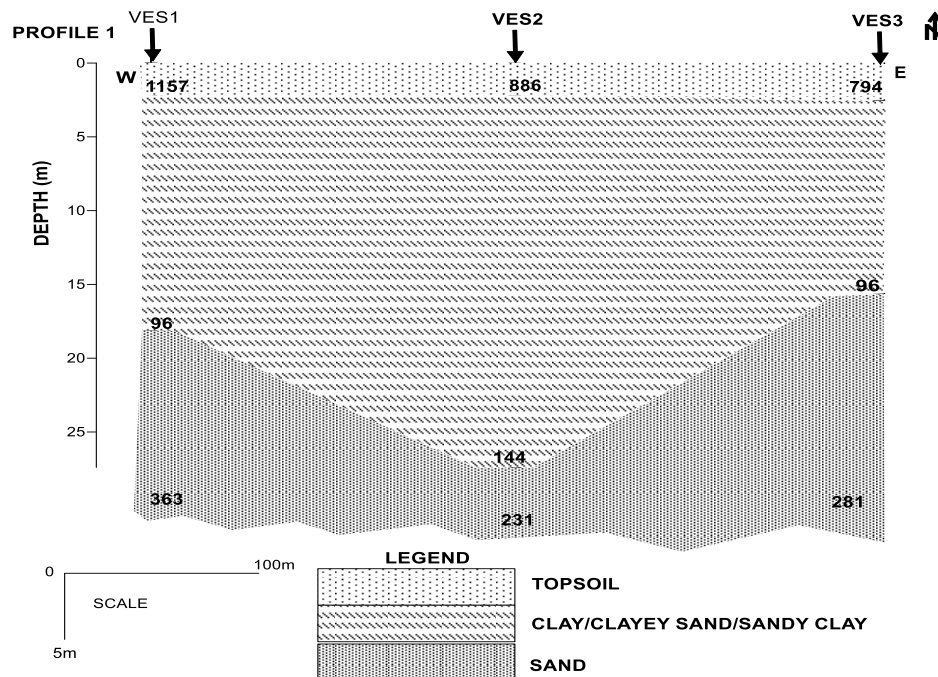


Figure 26. Geoelectric Section along Profile One

4.5.2.2. Geoelectric Section along Profile Five

The geoelectric parameter and layer sequence/lithology across profile five (Figure 27), revealed that the study area was characterized by three lithology/layer sequences comprising of resistive topsoil horizon with layer resistivity between 586 to 814 Ω m and layer thickness of less than 2.0 m, followed by a very weak/vulnerable second layer with layer resistivity of 121 Ω m to a maximum of 270 Ω m and layer thickness of about 15 to 16 m. this was subsequently followed by a resistive sand/sandstone layer with resistivity which varied between 501 to 1075 Ω m.

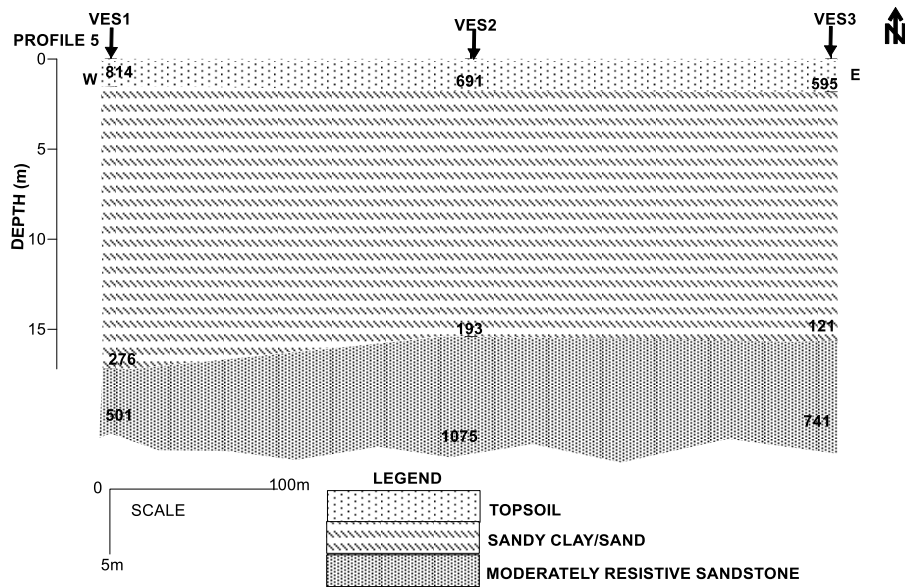


Figure 27. Geoelectric Section along Profile Five

4.5.2.3. Geoelectric Section along Profile Seven

In an attempt to have a better understanding of the geodynamics of the study area as it affects its vulnerability parameters, another control was engaged in traverse seven by carrying out three more Vertical Electrical Soundings (Figure 28). This further established the existence of three near surface layer occurrences, typical of the sedimentary environment of Nigeria. In this study, the topsoil comprises of highly resistive geologic materials of layer resistivity that ranged between 1038 to 1176 Ωm with a layer thickness of 5 m. followed by a middle/second layer that is suspected to be highly vulnerable with layer resistivity between 86 to about 268 Ωm and layer thickness between 16 to about 25 m. following this layer is a third layer that was characterized by highly resistive sand possibly sandstone with resistivity ranging from 414 to 1022 Ωm.

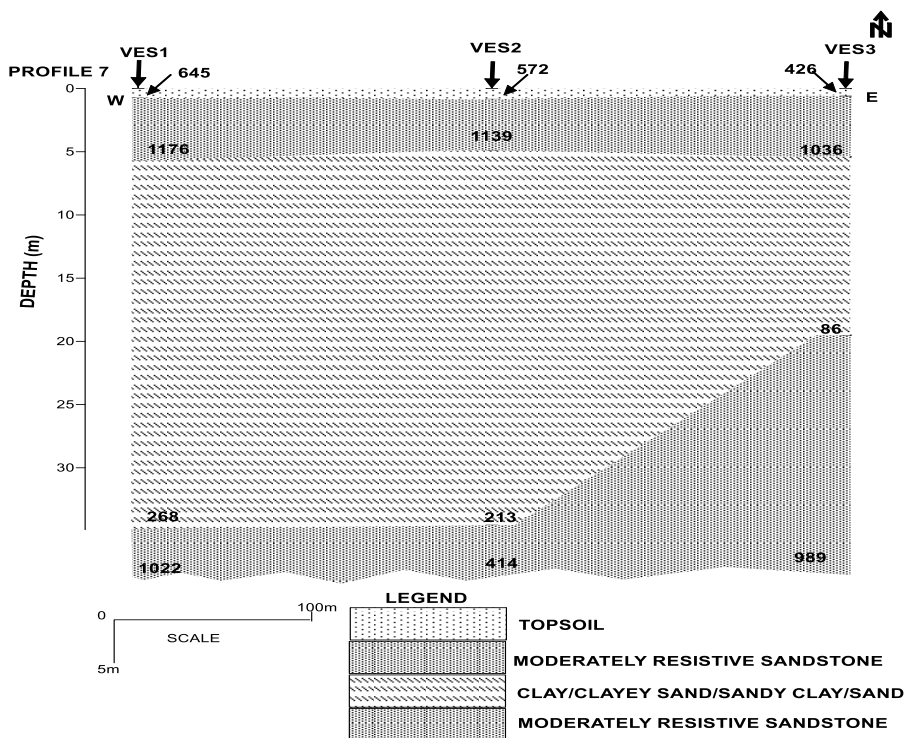


Figure 28. Geoelectric Section along Profile Seven

5.0. Conclusion

The investigation has justified the usefulness of deploying more than one methods and techniques in research work of this nature. The findings from the methods engaged in the study area was able to establish the major causes of the incessant collapse and failure of most foundations and civil engineering structures within the study area. This is unconnected with the existence of highly resistive materials. The occurrence of topsoil horizon materials of less than 2 m underlain by a weak vulnerable geologic material of layer thickness of an average of about 10 to 15 m, followed by a highly resistive layer. Therefore, since the load bearing capacity of the foundation of this area is largely dependent on the second layer which is highly incompetent from this study, it then becomes imperative that the ingenuity of the constructions and civil engineers must be brought into bearing for the sustainable and stability of any structure in this study area. All the methods engaged in this study exhibits an effective correlation and the area could be observed to be highly vulnerable to failure as a result of the inherent weak nature of the second layer. Due to the nature of the geologic settings of the study area, it is recommended that multi techniques and integrated geophysical approaches should be engaged in any engineering site constructions in the study area.

6.0. Data Availability Statement

The authors confirm that the data supporting the findings of the study are available within the article and its supplementary materials.

7.0. Conflict of Interest

Authors have declared that no competing interests exist and the data was not use as an avenue for any litigation but for the advancement of knowledge.

8.0. Funding

This research did not receive any specific grant from funding agencies in the public, commercial, or not-for-profit-sector.

9.0. Acknowledgement

The authors gratefully acknowledge Prof. A.O. Aina for his valuable contribution to improving the quality of this research work.

10.0. References

- [1] Morrow, C. A., Moore, D. E., Lockner, D. A. 2001. Permeability Reduction in Granite Under Hydrothermal Conditions. *Journal of Geophysics Research and Solid Earth*. Vol 106:30551-30560.
- [2] Bawallah M.A., Ayuks M.A., Ilugbo S.O., Ozegin K.O., Oyedele A.A., Aigbedion I., Aina A.O., Whetode J.M., Ladipo K.O., 2019a. Geodynamics and its implications to environmental protection: A case study of Aule area, Akure, Ondo State, Southwestern, Nigeria. *Applied Journal of Physical Science*, 1(3), 37-53.
- [3] Bawallah M.A., Oyedele A.A., Ilugbo S.O., Ozegin K.O., Ojo B.T., Olutomilola O.O., Airewele E., Aigbedion I. 2020a. Evaluation of structural defects and the dynamic of stress and strain on a building along Oluwole Area, Southwestern Nigeria. *Applied Journal of Physical Science*, 2(2), 23-37.
- [4] Aigbedion I., Bawallah M.A., Ilugbo S.O., Abulu F.O., Eguakhide V., Afuaman E.W., Ukubile B., 2019a. Geophysical Investigation for Pre-Foundation Studies at RCCG, Calvary Love Parish 2, Ukpenu, Ekpoma, Edo State, Nigeria, *International Journal of Research and Innovation in Applied Science (IJRIAS)*, 4(5), 39-45
- [5] Bawallah M.A., Adiat K.A.N., Akinlalu A.A., Ilugbo S.O., Akinluyi F.O., Ojo B.T., Oyedele A.A., Bamisaye O.A., Olutomilola O.O., Magawata U.Z. 2021a. Resistivity Contrast and the Phenomenon of Geophysical Anomaly in Groundwater Exploration in A Crystalline Basement Environment, Southwestern Nigeria, *International Journal of Earth Sciences Knowledge and Applications*, 3 (1) 23-36
- [6] Aigbedion I., Bawallah M.A., Ilugbo S.O., Ozegin K.O., ThankGod A., Atama J., Nwankwo B., Oladi O.O., Oladeji J.F., Alabi S.K., 2021. Environmental Impact Assessment of Structural Defects Using Geophysical and Geotechnical Methods in Parts of Ekpoma, Southsouthern Nigeria. *International Journal of Earth Sciences Knowledge and Applications*, 3 (2) 124-133
- [7] Sharma V. P., 1998. *Environmental and Engineering Geophysics*, published by Cambridge University Press, United Kingdom. Pp. 40 – 45.
- [8] Adebisi A.D., Ilugbo S.O., Ajayi C.A., Ojo A.O., Babadiya E.G., 2018. Evaluation of pavement instability section using integrated geophysical and geotechnical methods in a sedimentary terrain, Southern Nigeria. *Asian Journal of Geological Research*, 1(3), 1-13.
- [9] Bawallah M.A., Ilugbo S.O., Aigbedion I., Aina A.O., Oyedele A.A., 2019b. Modeling of subsurface integrity using Dar-Zarrouk parameters: A case study of Ikekogbe UBE Primary School, Ekpoma, Edo State, Nigeria. *Journal of Geography, Environment and Earth Science International*, 22(1), 1-17.
- [10] Aigbedion I., Bawallah M., Ilugbo S., Osaigbovo A.D., Diana E.K., Ihewkwumere C., Igbinoba C., Patrick P.U., Amagbamwan E. 2019b. Geophysical Investigation for Post Foundation Studies at Ikekogbe Primary School, Ekpoma, Edo State, Nigeria. *American Journal of Environmental and Resource Economics*. 4(2), 73-83. doi: 10.11648/j.ajere.20190402.14
- [11] Adebo B.A., Makinde E.O., Ilugbo S.O. 2021. Application of Electrical Resistivity Method to Site Characterisation for Construction Purposes at Institute of Agriculture Research and Training Moor Plantation Ibadan. *Indonesian Journal of Earth Sciences*, 1 (2), 49-62
- [12] Bawallah M.A., Adiat K.A.N. Akinlalu A.A., Ilugbo S.O., Akinluyi F.O., Benjamin O.O., Oyedele A.A., Omosuyi G.O., Aigbedion I. 2021b. Groundwater Sustainability and the Divergence of Rock Types in a Typical Crystalline Basement Complex Region, Southwestern Nigeria. *Turkish Journal of Geosciences*, 2 (1) , 1-11 . DOI: 10.48053/turkgeo.777217
- [13] Ilugbo S.O., Adebisi A.D., Olaogun S.O., Egunjobi T., 2018a. Application of Electrical Resistivity Method in Site Characterization along Ado – Afao Road, Southwestern Nigeria, *Journal of Engineering Research and Reports*, 1(4), 1-16.
- [14] Ilugbo S.O., Adebo A.B., Ajayi O.A., Adewumi, O.O., Edunjobi H.O., 2018b. Geophysical and geotechnical studies of a proposed structure at Akure, Southwestern Nigeria. *Journal of Engineering Research and Reports*, 2(2), 1-12.
- [15] Adebo B.A., Layade G.O., Ilugbo S.O., Hamzat A.A., Otobrise H.K., 2019. Mapping of Subsurface Geological Structures using Ground Magnetic and Electrical Resistivity Methods within Lead City University, Southwestern Nigeria, *Kada Journal of Physics*, 2 (2), 64-73
- [16] Bawallah M.A., Ilugbo S.O., Aina A.O., Olufemi B., Akinluyi F.O., Ojo B.T., Oyedele A.A., Olasunkanmi N.K. 2020b. Hydrogeophysical Studies of Central Kwara State Basement Complex of Nigeria. *International Journal of Earth Sciences Knowledge and Application* 2 (3) 146-164
- [17] Ajayi, C. A., Akintorinwa, O. J., Ademilua, L. O. 2020. Empirical Relationship between Gravimetric and Mechanical Properties of Basement Rocks in Ado-Ekiti, Southwestern Nigeria, *Journal of Geology and Geophysics*, 9(1):470.
- [18] Bawallah AM, Ilugbo SO, Adebo BA, Kehinde OA. 2021c. Geophysical investigation for detecting buried human remains after eight years of burial in Owo, Southwestern Nigeria. *J Forensic Sci*. 00:1-9. <https://doi.org/10.1111/1556-4029.14923>
- [19] Adebo B.A., Ilugbo S.O., Jemiriwon E.T., Ali A.K., Akinwumi A.K., Adeniken N.T. 2022. Hydrogeophysical Investigation Using Electrical Resistivity Method within Lead City University Ibadan, Oyo State, Nigeria. *International Journal of Earth Sciences Knowledge and Applications* 4(1), 51-62
- [20] Akinola, M. A., Akinlalu, A. A., Adelusi, O. A., 2017. Integrated Geophysical Investigation for Pavement Failure along a Dual Carriage Way, Southwestern Nigeria: A Case Study, *Kuwait Journal of Science*, 44(4): 135-149.

- [21] Ilugbo, S.O., Adebo, B.A., Olomo, K.O., Adebisi, A.D. 2018c. Application of GIS and multicriteria decision analysis to geoelectric parameters for modeling of groundwater potential around Ilesha, Southwestern Nigeria. *European Journal of Academic Essays* 5 (5), 105-123.
- [22] Ilugbo S.O., Adebisi A.D., A., Olomo K.O. 2018d. Modeling of groundwater yield using GIS and electrical resistivity method in a basement complex Terrain, Southwestern Nigeria. *Journal of Geography, Environment and Earth Science International*, 16(1), 1-17.
- [23] Ilugbo, S.O., Adebisi, A.D. 2017. Intersection of lineaments for groundwater prospect analysis using satellite remotely sensed and aeromagnetic dataset around Ibodi, Southwestern Nigeria. *International Journal of Physical Sciences*, 12(23), 329-353.
- [24] Ilugbo S.O., Edunjobi H.O., Adewoye O.E., Alabi T.O., Aladeboyeje A.I., Olutomilola O.O., Owolabi D.T. 2020. Structural Analysis Using Integrated Aeromagnetic Data and Landsat Imagery in a Basement Complex Terrain, Southwestern Nigeria. *Asian Journal of Geological Research*, 3(2): 17-33
- [25] Reyment, R. A. 1965. *Aspects of the Geology of Nigeria*. University of Ibadan Press, Ibadan.132pp
- [26] Allen, J. R. L. 1965. Late Quaternary Niger Delta and Adjacent Areas: Sedimentary Environments and Lithofacies. *Bulletin American Association of Petroleum Geology* vol. 49(5), pp. 547-600.
- [27] Burke, K., Dessauvage, T.F.J., Whiteman, A.J. 1971. Opening of the Gulf of Guinea and Geophysical History of the Benue Depression and Niger Delta Basin. University of Ibadan Press, Ibadan, Nigeria, 233: 51-53pp.
- [28] Murat, R. C. 1970. Stratigraphy and Paleogeography of the Cretaceous and Lower Tertiary in Southern Nigeria: In *African Geology*. University of Ibadan Press, 635-648
- [29] Fraser, D.C. 1969. Contouring of VLF-EM data. *Geophysics*, vol.34, 958-967.
- [30] Vander-Velpen B. P. A. 2004. WinRESIST Version 1.0 Resistivity Depth Sounding Interpretation Software. M. Sc Research Project, ITC, Delft Netherland.
- [31] Ghosh, D.P. 1971. The application of linear filter theory to the direct interpretation of geoelectrical resistivity sounding measurements. *Geophys. Prospecting* 19:192-217.
- [32] Akintorinwa O. J., Adeusi F. A. 2009. Integration of Geophysical and Geotechnical Investigations for a Proposed Lecture Room Complex at the Federal University of Technology, Akure, SW, Nigeria. *Ozean Journal of Applied Sciences* 2(3):1943-2429
- [33] Barker, F., Nagano, S., Ohmi, M., 1996. Lineaments analysis of satellite images using a Segment Tracing Algorithm (STA): *Computers and Geosciences*, V. 21, PP. 1091-1104.
- [34] Karous M, Hjelt S.E, 1983. Linear-filtering of VLF dip-angle measurements. *Geophysics. Prospecting*, 31: 782-894.
- [35] Kunetz, G. 1966. Principles of Direct current prospecting. *Geophys. Monogr.* 1(1):103.
- [36] Obi, G. C. 2006. Depositional Environment of Ajali Sandstone – Anambra Basin, Southeastern Nigeria. *Nigerian Mining Geology Journal*. Volume 6(3): 96 – 113pp
- [37] Ozegin K.O., Bawallah M.A., Ilugbo S.O., Oyedele A.A., Oladeji J.F., 2019. Effect of geodynamic activities on an existing dam: A case study of Ojirami Dam, Southern Nigeria. *Journal of Geoscience and Environment Protection*, 7(9), 200-213.
- [38] Philip Kearey, Michael Brooks and Ian Hill 2002. *An introduction to geophysical exploration*. Blackwell Science Limited, pp 225-228.
- [39] Reynold, J.M. 1997. *An introduction to Applied and Environmental Geophysics*. John Willy and Sons second edition.
- [40] Telford, W.M., Geldart, L.P., Sheriff, R.E., Keys, D.A. 1990. *Applied geophysics*, 2nd Edn., Cambridge University Press.
- [41] Telford, W.M., Geldart, L.P., Sheriff, R.E., Keys, D.A. 1976): *Applied geophysics*, 2nd Edn., Cambridge University Press, USA, pp: 113 – 114.